

ASSEMBLY OF THE TAIL OF BACTERIOPHAGE T4

Yoshiko Kikuchi and Jonathan King

Department of Biology, Massachusetts Institute of Technology, Cambridge, Massachusetts 02139

The protein products of at least 21 phage genes are needed for the formation of the tail of bacteriophage T4. Cells infected with amber mutants defective in these genes are blocked in the assembly process. By characterizing the intermediate structures and unassembled proteins accumulating in mutant-infected cells, we have been able to delineate most of the gene-controlled steps in tail assembly. Both the organized structures and unassembled proteins serve as precursors for *in vitro* tail assembly.

We review here studies on the initiation, polymerization, and termination of the tail tube and contractile sheath and the genetic control of these processes. These studies make clear the importance of the baseplate; if baseplate formation is blocked (by mutation) the tube and sheath subunits remain essentially unaggregated, in the form of soluble subunits.

Seventeen of the 21 tail genes specify proteins involved in baseplate assembly. The genes map contiguously in two separate clusters, one of nine genes and the other of eight genes. Recent studies show that the hexagonal baseplate is the end-product of two independent subassembly pathways. The proteins of the first gene cluster interact to form a structure which probably represents one-sixth of the outer radius. The products of the other gene cluster interact to form the central part of the baseplate.

Most of the phage tail precursor proteins appear to be synthesized in a non-aggregating form; they are converted to a reactive form upon incorporation into pre-formed substrate complexes, without proteolytic cleavage. Thus reactive sites are limited to growing structures.

INTRODUCTION

The structurally distinctive tail of bacteriophage T4 has a well defined – though not well understood – biological function: the delivery of the viral chromosome through the cell envelope into the host cytoplasm. This complex, multistep process begins with the adsorption of the phage to the host cell via the long tail fibers (1). The hexagonal baseplate is then activated to make firm contact with specific host surface receptors, followed by a major conformational change of the baseplate from a hexagon into a six-pointed star with concomitant breaking of the bonds between tube and baseplate and triggering of sheath contraction. This then forces the released tail tube tip through the cell envelope. This sequence can be seen in the electron micrographs of Simon and Anderson (2, 3), and other steps can be deduced from experiments of Benz and Goldberg (17) and Male and Kozloff (19). Clearly the tail is a cocked, metastable structure, waiting to find the proper

Presented at the 1974 Squaw Valley Symposium on Assembly Mechanisms.

site on a cell surface. It is extremely stable to the range of temperature, pH, and ionic strength found in sewers, soil, and stomachs, but can still, upon a subtle interaction signal, rapidly and irreversibly engage in a rearrangement of most of its protein molecules.

From work on the characterization of amber- and temperature-sensitive mutants of T4, we know that the products of at least 21 (5, 6) phage genes are needed for the assembly of a complete phage tail. High-resolution SDS (sodium dodecyl sulfate) gel electrophoresis (7) has enabled us to show that most, though not all, of these gene products become structural proteins of the tail (8, 9). Folic acid and dihydrofolate reductase are also components of the tail (19, 27). We have been trying to understand the mechanisms by which these more than 20 different protein species interact to form a phage tail organelle. Our understanding of the normal assembly process has derived from analysis of phage mutants defective in tail assembly. Analysis of the structures which accumulate in cells infected with mutants defective in tail assembly has revealed that the formation of the phage tail involves a sequential protein interaction pathway (6, 12). The mutant-infected cells accumulate structures which are intermediates in the normal pathway and represent the last stable intermediate before the blocked step. The baseplate is assembled first in the sequence; when it is complete, the tail tube subunits polymerize on it. After initiation of tube polymerization, the sheath assembles on the baseplate around the tail tube, and finally a structure is added at the tip of the tail which forms the site for head attachment (6, 11). Note that the structural proteins are synthesized simultaneously; it is the interactions of the proteins that take place sequentially, not their appearance. The tail assembly pathway, with the proteins found in each structure, is shown in Fig. 1 and reviewed below. More detailed accounts can be found in references 6, 8, 9, and 11. The three dimensional reconstruction of the tail sheath is described in DeRosier and Klug (29). The complexity of the baseplate is shown clearly by the computer filtered electron micrographs in Crowther and Amos (21).

Of particular importance is the fact that the phage tail can be assembled *in vitro* from the components that accumulate in mutant-infected cells, as first described by Edgar and Wood (10). It is important to note that this is not a reconstitution system, as is ribosome *in vitro* assembly. The proteins forming the phage tail in the *in vitro* complementation system are true precursors which have never been part of the mature structure. In fact, we find that such precursor proteins are quite soluble and have little or no tendency to aggregate unless the proper substrate is present, as described below. They appear to be synthesized in a nonaggregating form and require activation by incorporation into some preformed structure followed by a presumed allosteric conformational change.

Sheath Assembly

If cells are infected with mutants blocked in phage head assembly, they accumulate free tail structures, which we take to be complete tails awaiting a head. These structures sediment at 130 S and can be easily isolated from free proteins by sucrose gradient centrifugation. Cells infected with phage mutants of gene 3, 15, or 18 accumulate tail structures which sediment at 80 S. These structures lack the tail sheath and consist of just the tail tube attached to the baseplate. However, if the cells infected with mutants in gene 3 or 15 are examined immediately after cell lysis, most of the tails have a considerable length of sheath, but the sheath subunits fall off sequentially from the neck end, yielding 80 S

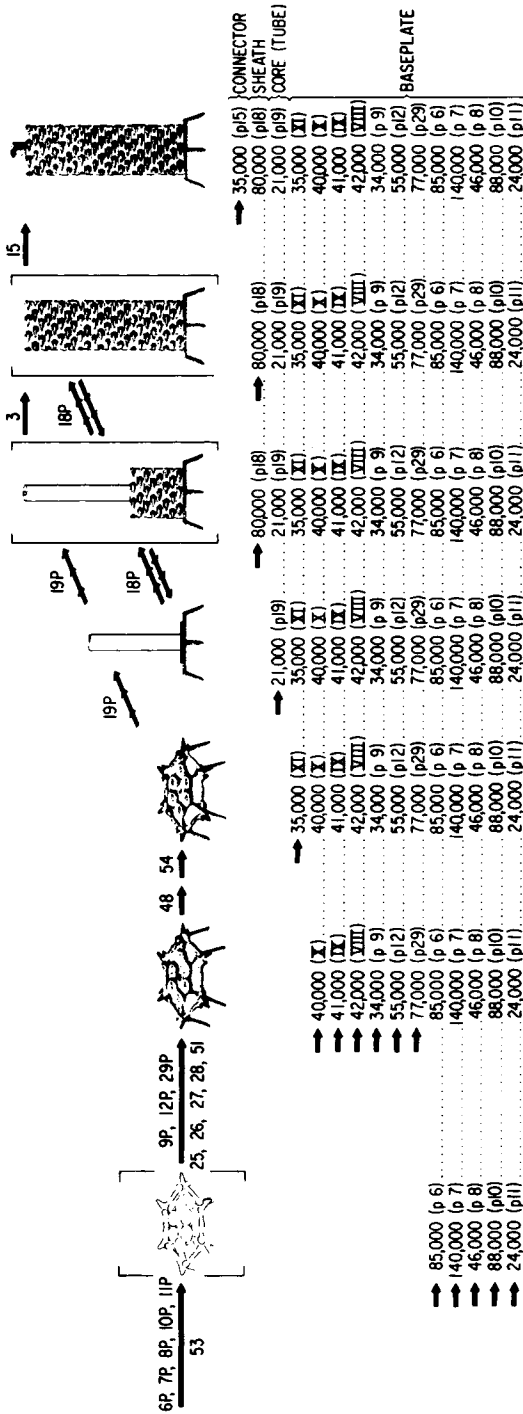


Fig. 1. Sequential pathway of T4 tail core and sheath assembly. The columns under each structure show the proteins found in each structure and their molecular weights as determined by SDS acrylamide gel electrophoresis (8, 9). For proteins which have been genetically identified, the number in parentheses is the name of the gene specifying that protein. In the pathway, gene products are labeled with a capital "P," since the functional protein may be a multimer. In general, if a step is blocked due to mutation, the intermediate structure accumulates, while the subsequent proteins in the pathway remain unaggregated. That is, the soluble proteins do not interact with each other but only with the growing structure. The baseplate assembly pathway is not linear, as suggested in the figure, but branched, as described in the text. The structure shown in brackets probably represents an aberrant side-product of assembly.

naked tails. The products of genes 3 and 15 are needed for the stabilization of the completed sheath, rather than for sheath polymerization. In fact, careful examination of complete tails shows that they are about 10% longer than tube baseplates, the extra length being due to a small protrusion from the end of the tail, called the connector. The gene 18 product, MW 80,000, has been shown to be the subunit of the sheath, while the gene 15 product forms the small connector, the site for head attachment (9). This structure does not form on the tip of the tail tube unless sheath polymerization is complete (6, 9, 11). The metastable contractile sheath is thus formed by a two-stage process: (1) A reversible polymerization of sheath protein monomer around the tail tube and (2) fixation of the structure by the formation of a special tube-sheath bond at the terminus of the tail (11).

During contraction all the subunits of the sheath must slide past the tube subunits, except the top annulus, which must be firmly bonded to the top of the tail if the sheath contraction is to force the tail tube through the host cell envelope. What is it that distinguishes the top annulus from all the others, permitting only it to be firmly bonded to the tail tube? The gene 3 product appears to add to or form the top annulus of the tail tube to make it a substrate for the formation of the connector. The connector, made of P15,¹ actually joins the top annulus of the sheath to the top annulus of the core (6, 9, 11). Of course, this raises the question of how P3 recognizes only the last annulus of the tube in the first place. As discussed in the next section, we suspect that an extended protein specifies the length of the tail tube and that P3 interacts with the terminus of this molecule.

Assembly of the Tail Tube

Cells infected with mutants in any of 12 tail genes fail to form baseplates (6). Lysates of these infected cells lack tail tubes, indicating that the tail tube forms only on the phage baseplate. Analysis of the lysate proteins shows that the tail tube protein – the product of gene 19 – is present in all these lysates (8), apparently in an unassembled form. If mutant extracts lacking baseplates but containing P19 are mixed together with 19⁻ extracts, which lack the tube protein but contain complete baseplates, viable phage are formed (11). This *in vitro* complementation result shows that the unassembled P19 is functional and serves as a precursor when provided with substrate baseplates. Apparently tail tube protein cannot polymerize in the absence of the baseplate, which must either provide a nucleation site for polymerization or induce a conformational change in tube subunits which bind to it, converting them to reactive sites for further polymerization. This is discussed in greater detail in King (11) and King and Mykolajewycz (9).

Cells infected with mutants of genes 48 or 54 accumulate morphologically normal baseplates and unassembled tube subunits. These gene products behave formally as initiator proteins for tube polymerization. We have found that the gene 48 and 54 proteins are incorporated into the baseplate (Kikuchi and King, unpublished experiments; also P. Berget and H. Warner, personal communication).

The mechanism of tail-length determination is not known. Tail tubes formed either *in vivo* or *in vitro* are never longer than 1,000 Å. Experiments of Moody (13) show that they are composed of 24 annuli of six subunits each. We have shown by comparison of

¹ A "P" before a gene number specifies the protein product of that gene.

the protein composition of free baseplates with tube-baseplates that P19 is the only major component of the tube (9). In vitro complementation experiments show that tube assembly is not sensitive to RNase or DNase, making it unlikely that the length is determined by an RNA or DNA molecule, in exact analogy to TMV. We suspect that a long protein chain or chains specifies the length of the tail. However, we have not yet been able to directly establish the existence of such a length-determining protein.

Baseplate Assembly

The baseplate is the most complex part of the phage tail. As can be seen from Fig. 1, most of the tail proteins are in fact structural proteins of the baseplate. The baseplate genes map in two clusters; the first contains genes 53-5-6-7-8-9-10-11-12, in that order, and the second contains genes 25-26-51-27-28-29-48-54, also in that order. The first cluster genes specify the major structural proteins of the baseplate (8, 9). The second cluster genes probably specify minor or catalytic proteins (8, 15, 16). We describe below some experiments which suggest that the baseplate is assembled via two pathways, one forming the central part and the other forming the repeating outer part. The first cluster gene products, the major proteins, are predominantly involved in the repeating structure, while the second cluster gene products are predominantly involved with the central part.

METHODS

Preparation of Defective Lysates

Phage and bacterial strains have been described previously (8, 10). ^{14}C -labeled defective lysates were prepared as follows. *E. coli* Bb was grown to 4×10^8 per ml in M9 (8) minimal medium at 30°C . Twenty-five ml of the culture were infected (m.o.i. = 5) with phage carrying an amber mutation of interest. The phage also carried amber mutations in gene 23, which specifies the major head protein, to prevent the formation of head-related structures in these lysates. The cultures were superinfected at 12 min after infection at the initial multiplicity. At 30 min ^{14}C -amino acid mixture was added ($0.1\text{--}2.0\ \mu\text{C}/\text{ml}$) and then chased with 1% casamino acids at 40 min. The cells were collected before lysis by centrifugation at 45 min. The pellet was suspended in phosphate buffer (1/10 M9, 5 mM MgSO_4 , pH 7.4) and DNase (20 $\mu\text{g}/\text{ml}$), and then frozen at -70°C .

After thawing, the lysate was incubated at 30°C for 10 min and further for 20 min with RNase (20 $\mu\text{g}/\text{ml}$) and 10 mM EDTA to degrade ribosomes. After removing cell debris by centrifugation, the supernatant was used for further analysis.

Preparation of Extracts for In Vitro Complementation

E. coli Bb was grown to 4×10^8 per ml in LB (26), 20 mM MgSO_4 at 30°C (200 ml), and infected with amber mutant of interest [double mutant with t gene (14)] at m.o.i. = 5. Sixty min later the culture was centrifuged before lysis. The pellet was frozen at -70°C . BUM (0.1 ml, 1/10 M9, 20 mM MgSO_4 , pH 7.4) and 0.03 ml of DNase (5 mg/ml) was added during thawing. We used this crude extract for in vitro complementation assay.

Acrylamide Gel Electrophoresis and Autoradiography

Samples were mixed with equal volumes of sample buffer, heated in boiling water for several minutes to dissociate structures, and electrophoresed through a 10% acrylamide slab gel; the gel was then dried for autoradiography, as described previously (8). These materials were composed as follows: sample buffer – 10% glycerol, 5% mercaptoethanol, 3% SDS, 0.0625 M Tris-HCl (pH 6.8), Brom Phenol Blue; stacking gel – 3.8% acrylamide gel (bis,¹ 0.1%), 0.125 M Tris-HCl (pH 6.8), 0.1% SDS, 0.1% TEMED,² 0.03% ammonium persulfate; separating gel – 10% acrylamide gel (bis, 0.26%), 0.375 M Tris-HCl (pH 8.8), 0.1% SDS, 0.05% TEMED, 0.05% ammonium persulfate; running buffer – Tris 3.03 gm, glycine 14.4 gm, SDS 1 gm/l.

RESULTS

Having defined the pathway for the formation of the tail tube and sheath, we focused our attention on the formation of the baseplate. In particular we wanted to know the structural precursors for the putting together of the baseplate. Is it assembled from six wedges? From an outer ring, an inner ring, and a central plug? From spikes projecting out of a central plug and then cross bridges added?

To this end we prepared ¹⁴C-amino-acid labeled lysates of cells infected with mutants defective in baseplate assembly. The lysates were centrifuged through sucrose gradients to detect accumulated structures that might be related to precursors of baseplates. From the distribution of radioactivity in such gradients, the baseplate-defective mutants could be divided into two classes. Group II mutant lysates display a 70 S peak, often with a shoulder trailing to a 40 S peak (Fig. 2). Each of these lysates also displays a peak of radioactivity at 15 S. Group I mutant lysates – 6⁻, 7⁻, 8⁻, 10⁻, and 53⁻ – do not contain any labeled structures sedimenting more rapidly than about 15 S. Centrifugation for longer times shows that some of the Group I lysates do contain distinctive labeled peaks. 53⁻ defective lysates accumulate a 15 S structure, 6⁻ lysates accumulate a 13 S structure, and 8⁻ lysates accumulate a 12 S structure. Most of the phage protein in lysates sediments from 2–9 S, with the leading edge composed of tail fibers. 7⁻ and 10⁻ lysates display no peak faster than 9 S, so almost all the tail proteins in the lysates are presumably sedimenting with the rest of the free proteins. SDS gel electrophoresis of the sucrose gradient fractions shows quite clearly that the unassembled precursor proteins do not aggregate (Kikuchi and King, in preparation). Figure 3 shows typical examples of the different sedimentation patterns.

Protein Composition of Incomplete Structures

The 70 S fractions from the Group II mutant lysates were dissociated in hot SDS and electrophoresed through an acrylamide gel. All the 70 S peaks contain all the major baseplate components: P7, P10, P6, P12, P8, P9, and P11. They lack, however, a number of the minor components. Figure 4 shows the pattern of radioactive protein bands from gels of completed baseplates from a 19⁻ lysate, and from gels of the 70 S and 40 S peaks of a 5⁻ lysate. The 5⁻ 70 S structure differs only in minor proteins from

¹bis: N, N'-methylene-bisacrylamide

²TEMED: N, N, N', N'-tetra-methylethylenediamine

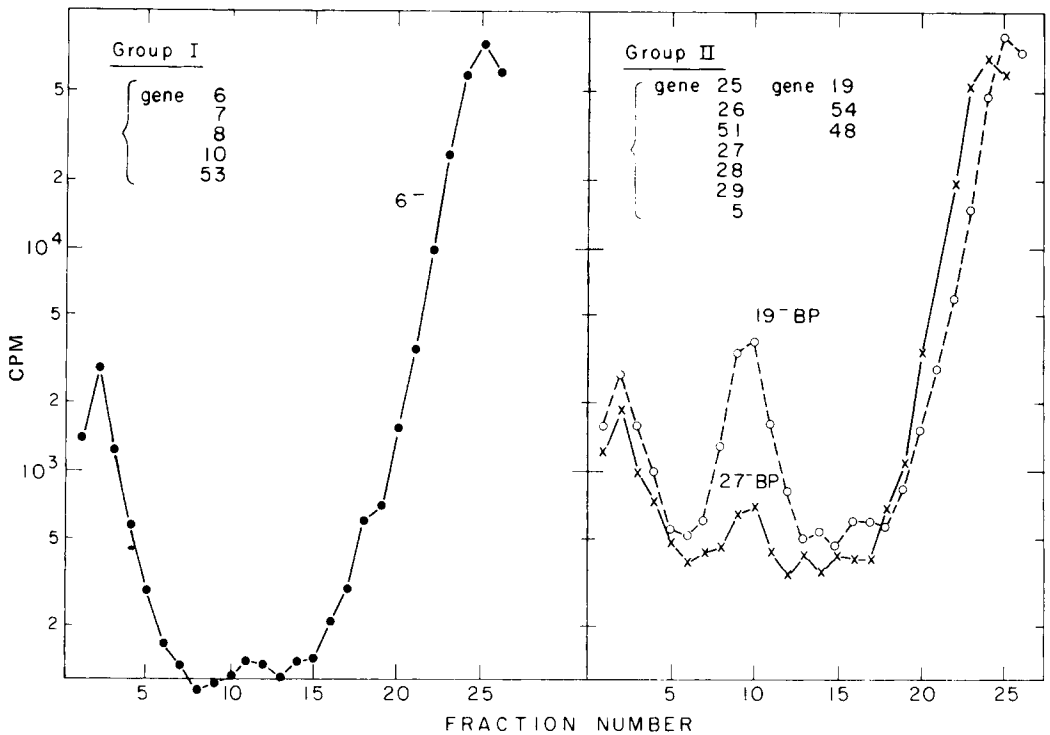


Fig. 2. Sucrose gradient centrifugation of baseplate defective structures. Lysates of amber mutant infected cells were prepared as described in Methods. The supernatants were centrifuged through 5–20% linear sucrose gradients in phosphate buffer, with 60% sucrose cushion at the bottom, for 80 min at 45,000 rev/min. Aliquots of 25 μ l of each fraction were counted in Triton X-100-based scintillation fluid. “Bp” is short for baseplate. Baseplates sediment at around 70 S.

the 19⁻ 70 S baseplates. The 5⁻ 40 S structure, however, is somewhat deficient in two major proteins, P9 and P12. We suspect that the 40 S structures are breakdown products of the 70 S baseplates; electron microscopic examination, described below, supports this idea. The peak to the left of P6 in the center panel of Fig. 4 is P18, the sheath protein, and is due to polysheath sedimenting in this region of the gradient.

The protein compositions of the 15 S structure accumulating in 53⁻ lysates (not shown here) and the 15 S structures present in each of the Group II lysates (which contain 70 S structures) are very similar to 19⁻ 15 S structures. Figure 5 shows that 19⁻ 15 S structures are made of P7, P10, P6, P8, and P11 at least. The 13 S structure from 6⁻ lysates has P7, P10, P8, and P11. The 12 S structure from 8⁻ lysate has only P7, P10, and P11 (no P6). From this protein composition we can formulate a very tentative pathway as follows: P7 + P10 + P11 \rightarrow 12 S + P8 \rightarrow 13 S + P6 \rightarrow 15 S. In the absence of P53, the 15 S structures are unable to form 70 S structures. The products of the genes of Group II do not seem to affect the above pathway, and presumably act either further along in the pathway or independently on a parallel branch. This is shown more clearly in the sections below.

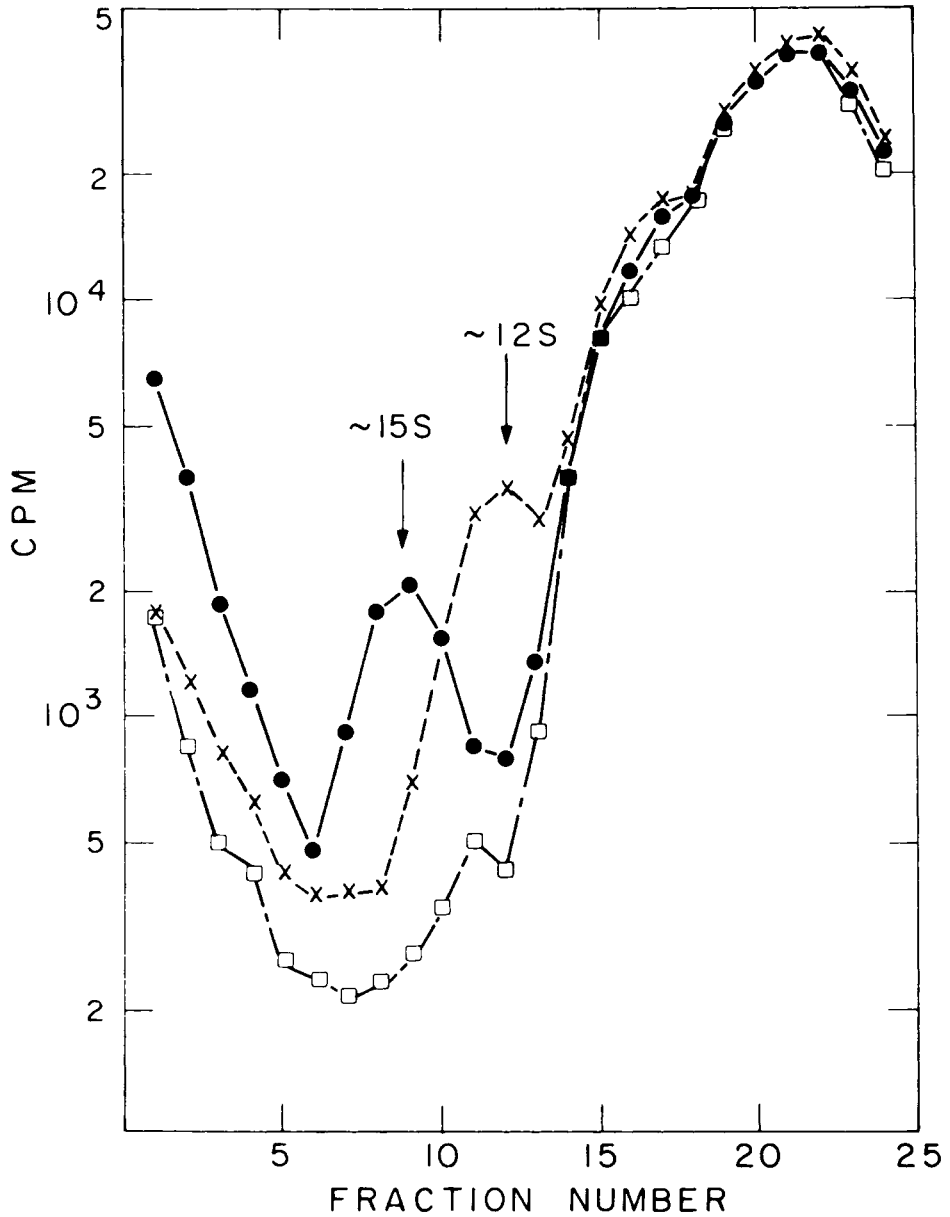


Fig. 3. Sucrose gradient centrifugation of baseplate defective lysates for longer times. The lysates were centrifuged at 45,000 rev/min for 7 hr at 4°C to separate protein complexes which might represent precursors of baseplates.

—●— 19⁻ lysate; —X— 8⁻ lysate; —□— 10⁻ lysate.

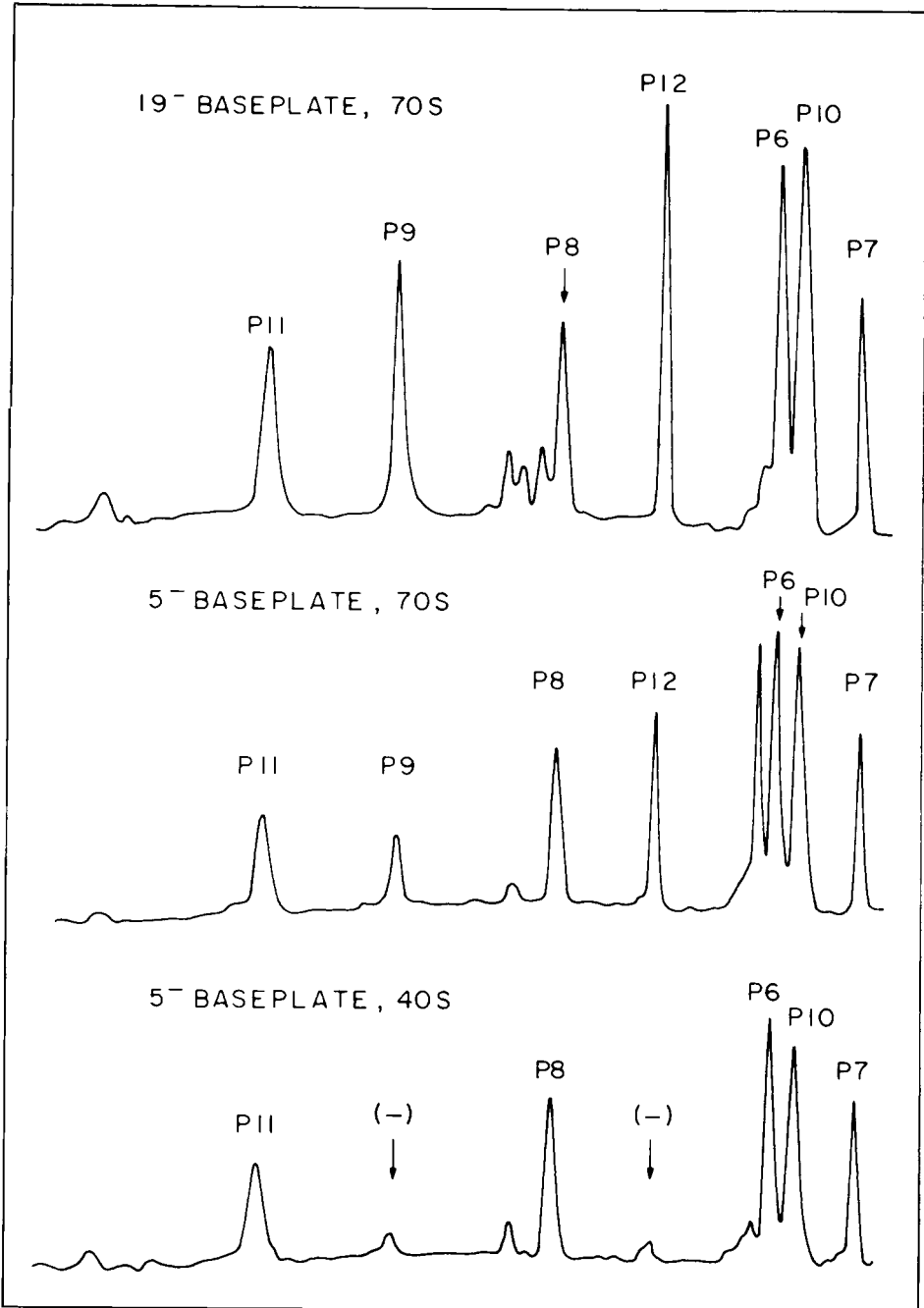


Fig. 4. Comparison of the protein compositions of base plate-related structures. Sucrose gradient fractions (shown in Fig. 2) were electrophoresed through 10% acrylamide gel, as described in Methods, and the gel was dried for autoradiography. Densitometer tracings of autoradiograms of the gels are shown.

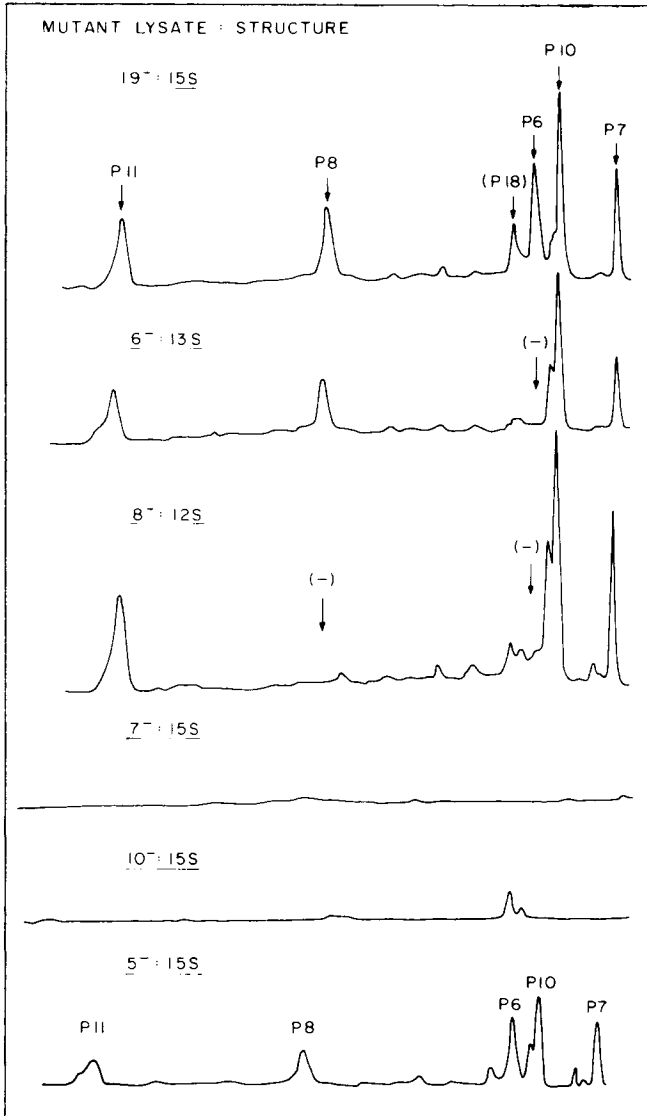


Fig. 5. Comparison of the protein compositions of slower baseplate-related structures. Sucrose gradient fractions from longer centrifugation (shown in Fig. 3) were electrophoresed, as described in

Electron Microscopy of Mutant Structures

Electron microscopic examination of the 70 S peaks from Group II mutant lysates revealed hexagonal baseplate-like structures, six-pointed-star structures which are apparently derived from hexagons, and amorphous lumps about the size of baseplates which we also presume are denatured hexagons. Figure 6 shows examples of those 70 S structures in comparison with complete baseplates from a 19⁻ defective (tube⁻) lysate.

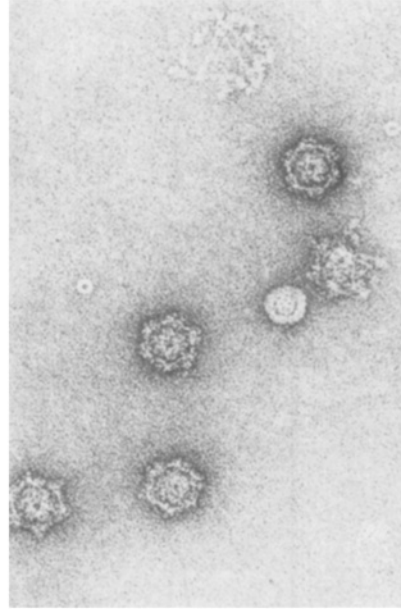
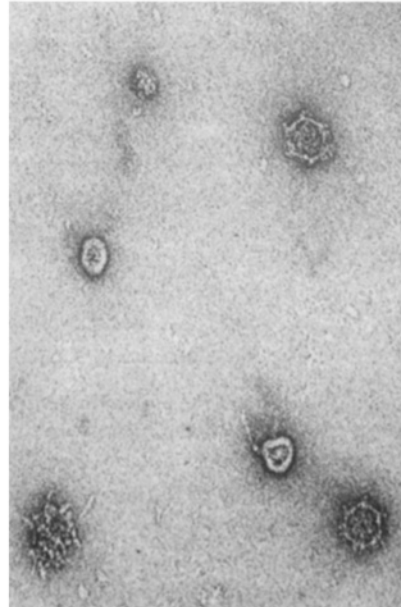
19⁻ BP5⁻ BP27⁻ BP51⁻ BP

Fig. 6. Comparison of electron micrographs of isolated baseplate structures. 70 S hexagonal baseplates from 5⁻, 27⁻, and 51⁻ lysates are shown, compared with complete 19⁻ baseplates.

The mutant structures appear to be missing the plug that is present in the center of the complete baseplate. The structures from the 40 S peaks generally appeared as amorphous lumps and six-pointed stars. Thus the Group II mutants appear to accumulate unstable hexagons which convert to six-pointed stars. We suspect that this conversion mimics the transition that the baseplate of a wild-type phage goes through during the infection process. The absence of the plug from 5⁻, 27⁻, and 29⁻ hexagons suggests that P5, P27, P29 are required for the formation of the plug in the complete baseplate.

In Vitro Complementation

Initial experiments to obtain baseplate formation in vitro by mixing extracts of cells infected with different mutants blocked in baseplate assembly were not reproducibly successful. Subsequently we constructed double mutants (28) between an amber in each of the tail genes and a T4 mutant in gene *t* which delays lysis (14) and results in continued protein synthesis. In mixtures of extracts made with such double mutants complementation is reasonably efficient, showing that baseplates and complete phage are forming in the extract mixture (Fitten and King, unpublished). In particular viable phage are formed in vitro on mixing 53⁻ extracts with extracts made from other Group I genes. We were therefore able to test whether the 15 S structure isolated from 53⁻ extract was the active intermediate in the reaction by measuring its ability to complement other Group I defective extracts. The results were positive (Table I), showing that the 15 S structure probably represents a normal intermediate in baseplate assembly.

The 70 S structures from Group II defective extracts were also tested for in vitro complementation activity. In these cases the results were uniformly negative. Either the 70 S structures are aberrant assembly products or they are extremely labile and are inactivated during preparation. In fact, we suspect the former is the case. The amount of 70 S + 40 S radioactivity from Group II defective lysates is substantially lower than that from the control 19⁻ baseplates, consistent with the idea that these structures form only inefficiently in infected cells.

TABLE I. Biological Activities of 15 S Structures from 53⁻ Lysate, Assayed by In Vitro Complementation

	7 ⁻ / t ⁻ extract (phage/ml)	8 ⁻ / t ⁻ extract (phage/ml)	10 ⁻ / t ⁻ extract (phage/ml)
53 ⁻ / t ⁻ supernatant	3.6 × 10 ¹²	3.3 × 10 ¹²	2.5 × 10 ¹²
53 ⁻ / t ⁻ 15 S	3.0 × 10 ¹¹	3.3 × 10 ¹¹	1.4 × 10 ¹¹
Background of each extract	8.0 × 10 ⁹	2.0 × 10 ⁹	3.0 × 10 ⁹

53⁻ / t⁻ extract was centrifuged at 20,000 rev/min for 20 min to remove debris and unabsorbed phage, so the supernatant (sup) contained the soluble proteins. The supernatant was centrifuged through 15–30% linear sucrose gradient in BUM, at 45,000 rev/min for 3 hr at 15°C. 10 λ of each sucrose fraction was mixed with 25 λ of extract, incubated for at least 2 hr at 30°C, and plated on *E. coli* CR63 (Su⁺). The 15 S fraction had the highest activity in the gradient tested by 7⁻ / t⁻, 8⁻ / t⁻, or 10⁻ / t⁻ extract. The backgrounds of phage in 53⁻ / t⁻ supernatant and 15 S fraction were less than 10⁹ per ml.

DISCUSSION

We first discuss the assembly of the phage baseplate and then discuss the behavior of structural proteins in tail morphogenesis in comparison with some other experimental systems. Since the major structural proteins of 70 S baseplates are all represented in the 15 S precursor, the 15 S structure probably represents the repeating unit of the hexagonal baseplate. Since the baseplate has six-fold symmetry, we would expect it in fact to be one sixth of a baseplate. Unfortunately, we are not yet sure of its morphology. The proteins of this structure are all specified by genes which map in one cluster on the T4 chromosome 6-7-8-9-10 and 11. Our evidence shows that these proteins are not cleavage products of larger precursors (8).

A striking feature of the assembly process is that the proteins appear to be synthesized in a form which is nonaggregating. For example, P6, P8, and P10 are not complexed in the absence of P7. This suggests that steps in the assembly process per se activate the proteins for further assembly reactions. P8, for example, cannot react with P6 unless it has already interacted with P7 and P10. This interaction then activates it by some allosteric mechanism so that it will be reactive for the next step. This is probably the mechanism underlying the sequential pathway of the assembly process and preventing the formation of incorrect aggregates. In cells lacking a protein (due to mutation), the later proteins in the pathway remain free. The important point is that many of the proteins remain free without any aberrant aggregation in the cell, so their biological activities can be demonstrated by the *in vitro* complementation assay of Edgar and Wood (10). This *in vitro* complementation system differs from the ribosome reconstitution system. In the phage system the proteins being characterized are precursors, while in the reconstitution system they are the mature proteins.

In the absence of the products of genes 5 and 25–29, some of which have been identified as minor components of the complete baseplate, 70 S structures are formed inefficiently. These cannot be converted to phage *in vitro* and are probably aberrant structures. A number of these structures are missing the central plug of the baseplate, suggesting that the plug may be composed of these gene products. Gene dosage experiments of Snustad (15) suggest that the products of genes 26, 28, and 51 act catalytically in the assembly process. Kozloff and coworkers have presented evidence that the gene 28 product catalyzes the formation of the phage-specific folic acid which they found in the baseplate (16). They suggested that the complex of the folic acid with dihydrofolate reductase, which is also a structural component of the baseplate (19), is involved with the triggering of the baseplate conformational change upon infection. Thus we think of these minor proteins as constituting the machinery involved in the triggering of contraction. Recently, we have shown from *in vitro* complementation experiments that there is a complex which is composed of P5, P27, and P29. The formation of this active complex requires the products of genes 26, 28, and 51 (Kikuchi and King, in preparation).

A number of other workers have approached phage tail structure from the point of view of function, rather than assembly. For example, Benz and Goldberg (17) have characterized mature particles which have passed part way through the attachment process and are essentially intermediates, not in assembly, but in function. Baylor et al. (20), Dawes and Goldberg (4), and Yamamoto and Uchida (18) have isolated and characterized mutants which render the complete phage heat-sensitive. Many of their mutants map in

genes for tail proteins. Examination of the morphology of the heat-killed particles gives information as to the function of the mutant gene product in the phage particle. Thus, for example, particles carrying heat-sensitive mutations in genes 48 and 25 inactivate by contracting their tail sheath but leave the baseplate still attached at the tip of the tail core, suggesting that P48 and P25 may form bonds between the sheath and the baseplate (18). Hopefully, as studies of the assembly pathway and of the interactions among proteins in the complete structure proceed, we will be able to describe more fully the topological and functional relationships among the baseplate proteins. Image processing of electron micrographs of baseplates should contribute significantly to the solution of baseplate structure (21).

The only baseplate protein that has been purified is the product of gene 12 (22). This protein is directly involved in attachment to the host cell (6) and forms part of the short fibers of the baseplate (23, 24).

There have been many studies on the assembly of subunits derived from the breakdown of mature structures — for example, ribosomes, enzyme subunits, and microtubules. In the case of proteins which are cleavage products, such as virus coat proteins or pro-collagen, it is clear that the mature proteins are not the molecules which participated in the assembly process. In the case of proteins which are not known to be cleavage products, such as tubulin, ribosomal proteins, and phage tail proteins, this is less clear. However, in the phage tail case, because of the extensive analysis of mutants, we can characterize the true precursor proteins, which have not engaged in the assembly process. These proteins have no tendency to spontaneously aggregate; for example, the tail tube subunits do not polymerize at all in the absence of baseplates, but they do polymerize highly efficiently onto the growing end of an already initiated tail tube. This is analogous to the situation described for bacterial flagellin polymerization (25), in which incorporation into the growing flagellum results in a major conformational change of the subunit, which is then an active site for further subunit addition. Thus we think it likely that in order to avoid aggregation at the wrong place or wrong time, even structural proteins that are not activated by proteolytic cleavage can exist in at least two states, the precursor non-aggregating form and the incorporated form which has reactive sites for other proteins. In the phage tail and bacterial flagellar cases, the transition is triggered by the assembly process itself.

ACKNOWLEDGMENTS

We thank Elaine Lenk for help with the electron microscopes and Roni McCall for preparation of the manuscript. This research was supported by N.I.H. grant GM-17,980.

REFERENCES

1. Bishop, R., Conley, M. P., and Wood, W. B., *J. Supramol. Struc.* 2:196 (1974).
2. Simon, L. D., and Anderson, T. F., *Virology* 32:279 (1967).
3. Simon, L. D., and Anderson, T. F., *Virology* 32:298 (1967).
4. Dawes, J., and Goldberg, E. B., *Virology* 55:391 (1973).
5. Epstein, R. H., Bolle, A., Steinberg, C. M., Kellenberger, E., Boy de la Tour, E., Chevally, R., Edger, R. S., Sussman, M., Denhardt, G. H., and Lielausis, A., *Cold Spring Harbor Symp. Quant. Biol.* 28:375 (1963).

6. King, J., *J. Mol. Biol.* 32:231 (1968).
7. Laemmli, U. K., *Nature* 227:680 (1970).
8. King, J., and Laemmli, U. K., *J. Mol. Biol.* 75:315 (1973).
9. King, J., and Mykolajewycz, N., *J. Mol. Biol.* 75:338 (1973).
10. Edgar, R. S., and Wood, W. B., *Proc. Nat. Acad. Sci. Wash.* 55:498 (1966).
11. King, J., *J. Mol. Biol.* 58:693 (1971).
12. Edgar, R. S., and Lielausis, I., *J. Mol. Biol.* 32:263 (1968).
13. Moody, M. F., *Phil. Trans. Roy. Soc., London, B.* 261:181 (1971).
14. Josslin, R., *Virology* 40:719 (1970).
15. Snustad, D. P., *Virology* 35:550 (1968).
16. Kozloff, L. M., Lute, M., and Baugh, C. M., *J. Virol.* 11:637 (1973).
17. Benz, W. C., and Goldberg, E. B., *Virology* 53:225 (1973).
18. Yamamoto, M., and Uchida, H., *Virology* 52:234 (1973).
19. Male, C. J., and Kozloff, L. M., *J. Virol.* 11:840 (1973).
20. Baylor, M. B., Symonds, N., and Hessler, A., *Genetics* 52:539–551 (1965).
21. Crowther, R. A., and Amos, L. A., *J. Mol. Biol.* 60:123 (1971).
22. Mason, W. S., and Haselkorn, R., *J. Mol. Biol.* 66:445 (1972).
23. Kells, S., and Haselkorn, R., *J. Mol. Biol.* 83:473 (1974).
24. Yanagida, M., and Ahmad-Zadeh, C., *J. Mol. Biol.* 51:411 (1970).
25. Asakura, S., *Adv. in Biophys.* 1:99 (1970).
26. Levine, M., *Virology* 3:22 (1957).
27. Kozloff, L. M., Lute, M., Crosby, L. K., Rao, N., Chapman, V. A., and DeLong, S. S., *J. Virol.* 5:726 (1970).
28. King, J., Fitten, R., Mykolajewycz, N., and Floor, E., *Virus Research*:259 (1973).
29. DeRosier, D., and Klug, A., *Nature* 217:130 (1970).